Science Immunology
AAAS

# Supplementary Materials for

## SARS-CoV-2 Omicron-neutralizing memory B-cells are elicited by two doses of BNT162b2 mRNA vaccine

Ryutaro Kotaki *et al.*

Corresponding author: Yoshimasa Takahashi, ytakahas@niid.go.jp

DOI: 10.1126/sciimmunol.abn8590

**The PDF file includes:**

Figs. S1 to S5

**Other Supplementary Material for this manuscript includes the following:**

Table S1

# SARS-CoV-2 Omicron-neutralizing memory B-cells are elicited by two doses of BNT162b2 mRNA vaccine

**Authors:** Ryutaro Kotaki[1†], Yu Adachi[1†], Saya Moriyama[1†], Taishi Onodera[1†], Shuetsu Fukushi[2], Takaki Nagakura[1], Keisuke Tonouchi[1], Kazutaka Terahara[1], Lin Sun[1], Tomohiro Takano[1], Ayae Nishiyama[1], Masaharu Shinkai[3], Kunihiro Oba[4], Fukumi Nakamura-Uchiyama[5], Hidefumi Shimizu[6], Tadaki Suzuki[7], Takayuki Matsumura[1], Masanori Isogawa[1], Yoshimasa Takahashi[1*]

**Affiliations:**

[1]Research Center for Drug and Vaccine Development, National Institute of Infectious Diseases; Tokyo 162-8640, Japan.

[2]Department of Virology I, National Institute of Infectious Diseases; Tokyo 162-8640, Japan.

[3]Tokyo Shinagawa Hospital; Tokyo, 140-8522, Japan.

[4]Department of Pediatrics, Showa General Hospital; Tokyo, Japan

[5]Department of Infectious Diseases, Tokyo Metropolitan Bokutoh Hospital; Tokyo, Japan

[6]Department of Respiratory Medicine, JCHO Tokyo Shinjuku Medical Center; Tokyo, Japan

[7]Department of Pathology, National Institute of Infectious Diseases; Tokyo 162-8640, Japan.

[*]Corresponding authors.

Yoshimasa Takahashi

Research Center for Drug and Vaccine Development, National Institute of Infectious Diseases

Email: ytakahas@niid.go.jp

†These authors contributed equally to this work.

**SUPPLEMENTARY MATERIALS**

Fig. S1. Participant demographics.

Fig. S2. RBD-binding antibody titers and correlation to neutralizing activities.

Fig. S3. Flow cytometry gating strategy for RBD-binding $B_{mem}$ cells.

Fig. S4. Additional analyses on the vaccine-induced $B_{mem}$ cell subsets.

Fig. S5. S309 antibody binding to Omicron RBD

Supplemental Table S1: Raw data file (excel)

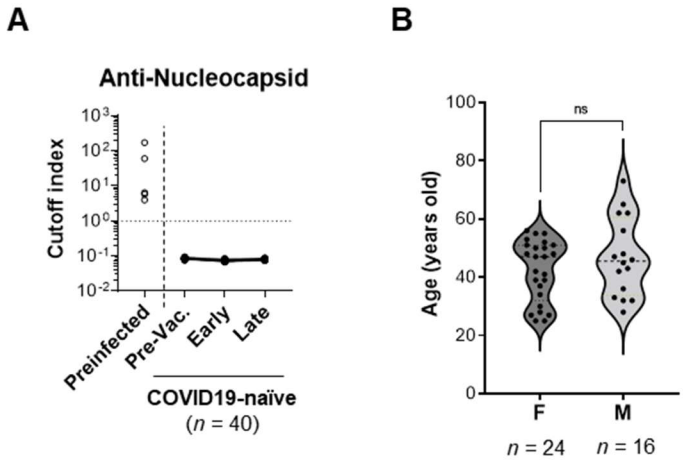


**Fig. S1. Participant demographics.**

(**A**) Anti-nucleocapside antibody titers of plasma collected prior to the first vaccination and at the early and late time points were measured. The dotted line on the y-axis indicates a detection limit (1.0) for the assay provided from the manufacturer. Samples with values above the detection limit at the pre-vac. time point were excluded from subsequent analyses. (**B**) Age distribution of the subjects was analyzed using the Mann-Whitney U-test (ns, not significant: $P \geq 0.05$).

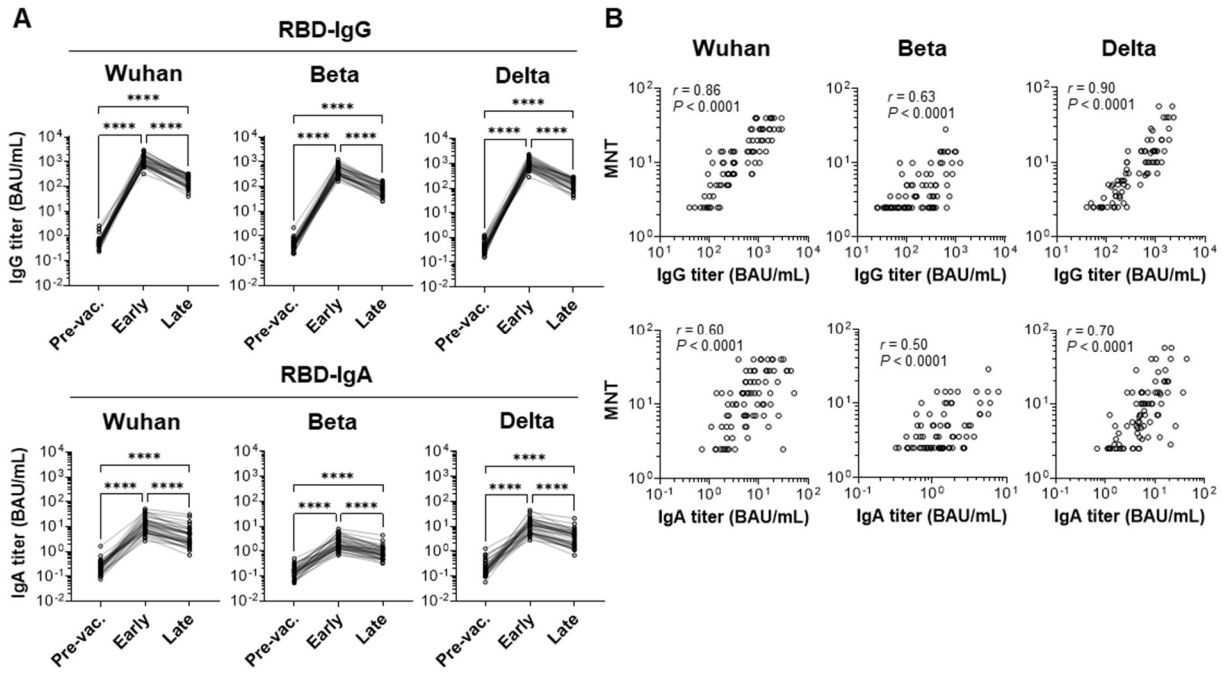


**Fig. S2. RBD-binding antibody titers and correlation to neutralizing activities.**

(**A**) Longitudinal RBD-binding IgG and IgA titers were measured using ECLIA. (**B**) Correlations between RBD-binding IgG or IgA and neutralizing titers were analyzed.

Statistical analyses were performed using the Friedman test (A) and Spearman's correlation analysis (B). ****$P < 0.0001$. Data were pooled from more than two independent experiments.

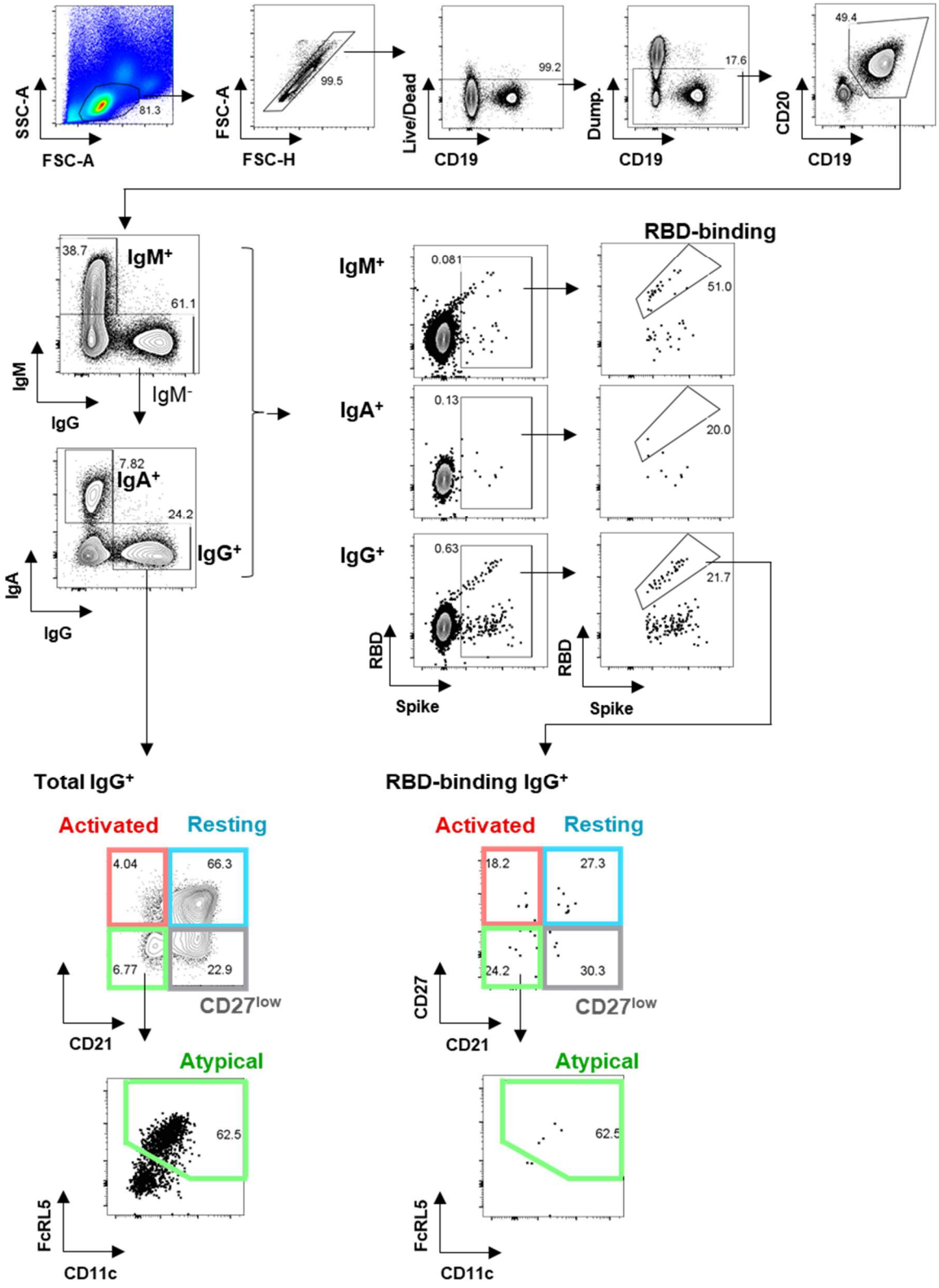
SSC-A
FSC-A
81.3
FSC-A
FSC-H
99.5
Live/Dead
CD19
99.2
Dump.
CD19
17.6
CD20
CD19
49.4
IgM
IgG
38.7
IgM+
61.1
IgM-
IgA
IgG
7.82
IgA+
24.2
IgG+
RBD-binding
IgM+
0.081
51.0
IgA+
0.13
20.0
IgG+
0.63
21.7
RBD
Spike
RBD
Spike
Total IgG+
RBD-binding IgG+
Activated
Resting
4.04
66.3
6.77
22.9
CD27low
CD21
Atypical
62.5
FcRL5
CD11c
Activated
Resting
18.2
27.3
24.2
30.3
CD27
CD27low
CD21
Atypical
62.5
FcRL5
CD11c

**Fig. S3. Flow cytometry gating strategy for RBD-binding $B_{mem}$ cells.**

RBD-binding IgM/IgA/IgG $B_{mem}$ cells were initially selected as $Dump^{-}CD19^{+}CD20^{+}$ cells and then divided into $IgM^{+}$, $IgA^{+}$, or $IgG^{+}$ cells. After gating on spike/RBD-binding cells, $IgG^{+}$ fractions were further delineated into $B_{mem}$ subsets based on CD21, CD27, CD11c, and FcRL5 expression as indicated in the plot. activated ($CD21^{-}CD27^{+}$), resting ($CD21^{+}CD27^{+}$), $CD27^{low}$ ($CD21^{+}CD27^{low}$), and atypical ($CD21^{-}CD27^{low}CD11c^{+}FcRL5^{+}$) subsets. Representative plots from four independent experiments are shown.

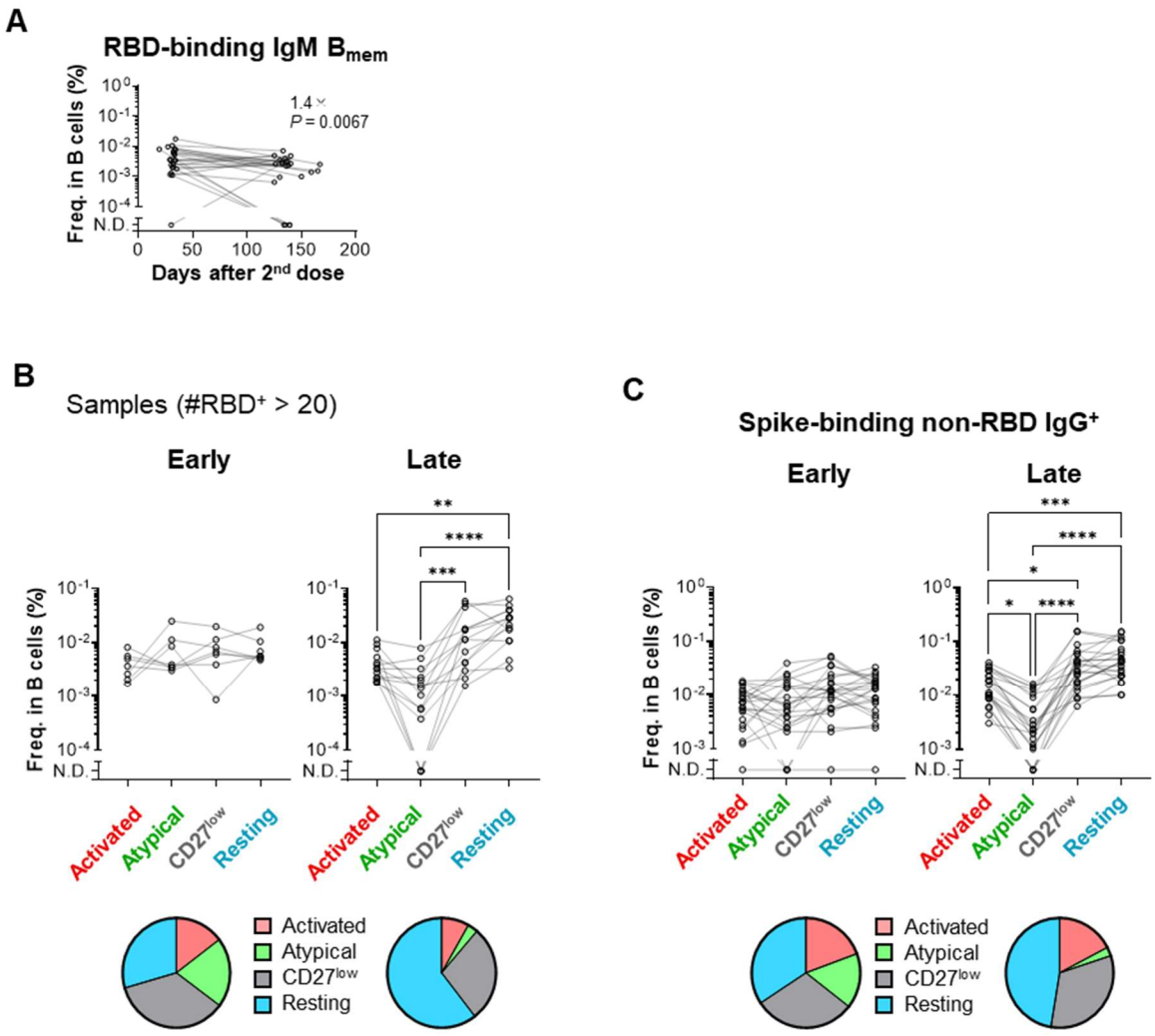


**Fig. S4. Additional analyses on the vaccine-induced $B_{mem}$ cell subsets.**

(**A**) Longitudinal frequencies of RBD-binding $CD21^+CD27^+$ IgM $B_{mem}$ cells among $CD19^+CD20^+$ B cells were analyzed ($n$ = 23). Values on the plots indicate fold decrease of median from the early to the late time points. (**B**) $B_{mem}$ cell subsets were analyzed using samples with >20 RBD-binding IgG $B_{mem}$ cells. In the pie charts, median frequency of $B_{mem}$ subsets among RBD-binding $IgG^+$ B cells were plotted (Early, $n$ = 7; Late, $n$ = 14). (**C**) $B_{mem}$ cell subsets were analyzed on Spike-binding, non-RBD-biding $IgG^+$ $B_{mem}$ cells ($n$ = 23). In the pie charts, median frequency of $B_{mem}$ subsets among RBD-binding $IgG^+$ B cells were plotted. Statistical

analyses were performed with the Wilcoxon test (A), and the Friedman test (B, C) (*$P < 0.05$, **$P < 0.01$, ***$P < 0.001$, ****$P < 0.0001$). Data were pooled from two independent experiments.

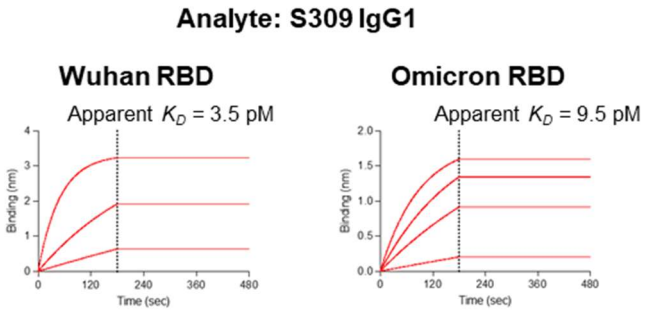


**Fig. S5. S309 antibody binding to Omicron RBD**

Binding of S309 IgG1 antibody to Wuhan-RBD (left) and Omicron-RBD (right) were quantitated with BLI. Biotinylated RBDs were captured on streptavidin-coated biosensors, and subsequently kinetics of S309 binding was analyzed. Signals were fitted to 1:1 binding model and apparent $K_D$ values were calculated. Representative data from two independent experiments are shown.